



OPEN

# Exploring the progression of drug dependence in a methamphetamine self-administration rat model through targeted and non-targeted metabolomics analyses

Sang-Hoon Song<sup>1,3</sup>, Suji Kim<sup>1,3</sup>, Won-Jun Jang<sup>1</sup>, In Soo Ryu<sup>2</sup>, Chul-Ho Jeong<sup>1</sup>✉ & Sooyeon Lee<sup>1</sup>✉

Persistent neurochemical and biological disturbances resulting from repeated cycles of drug reward, withdrawal, and relapse contribute to drug dependence. Methamphetamine (MA) is a psychostimulant with substantial abuse potential and neurotoxic effects, primarily affecting monoamine neurotransmitter systems in the brain. In this study, we aimed to explore the progression of drug dependence in rat models of MA self-administration, extinction, and reinstatement through targeted and non-targeted metabolomics analyses. Metabolic profiles were examined in rat plasma during the following phases: after 16 days of MA self-administration (Group M); after 16 days of self-administration followed by 14 days of extinction (Group MS); and after self-administration and extinction followed by a reinstatement injection of MA (Group MSM). Each group of MA self-administration, extinction, and reinstatement induces distinct changes in the metabolic pathways, particularly those related to the TCA cycle, arginine and proline metabolism, and arginine biosynthesis. Additionally, the downregulation of glycerophospholipids and sphingomyelins in Group MSM suggests their potential role in MA reinstatement. These alterations may signify the progressive deterioration of these metabolic pathways, possibly contributing to drug dependence following repeated cycles of drug reward, withdrawal, and relapse. These results provide valuable insights into the metabolic changes associated with MA use at various stages, potentially facilitating the discovery of early diagnostic biomarkers and therapeutic targets for MA use disorders.

**Keywords** Drug dependence, Methamphetamine, Self-administration, Reinstatement, Metabolomics, Mass spectrometry

According to the World Drug Report 2023, the number of drug users has progressively increased from an estimated 219 million in 2011 to 296 million in 2021, representing 5.8% of the global population aged 15–64 years. This signifies that one in every 17 individuals worldwide used drugs in 2021, 23% more than a decade earlier<sup>1</sup>. In particular, the number of individuals with drug use disorders was estimated at 39.5 million in 2021, reflecting a 45% increase from 10 years ago, with only 1 in 5 individuals receiving treatment<sup>1</sup>. The dysregulation of multiple neurotransmitter systems plays a key role in the development of drug use disorders. The initial or recreational administration of psychostimulants, such as methamphetamine (MA), immediately releases monoamines and reduces their reuptake, provoking a marked increase in their levels in extracellular spaces and excessive stimulation of the sympathetic nervous system. However, in rodents and non-human primates, repeated administration of increasing MA doses has been found to decrease striatal concentrations of dopamine and its metabolites. In human stimulant users, both the presynaptic and postsynaptic functions of the dopamine

<sup>1</sup>College of Pharmacy, Keimyung University, 1095 Dalgubeoldaero, Dalseo-gu, Daegu 42601, Republic of Korea.

<sup>2</sup>Biorchestra Co., Ltd, Techno4-ro 17, Daejeon 34013, Republic of Korea. <sup>3</sup>Sang-Hoon Song and Suji Kim contributed equally to this work. ✉email: chjeong75@kmu.ac.kr; sylee21@kmu.ac.kr

system in the striatum are downregulated<sup>2–4</sup>. These findings suggest that persistent neurochemical and biological disturbances, resulting from repeated positive and negative reinforcements associated with ongoing cycles of drug reward, withdrawal, and reinstatement, contribute to the development of drug use disorders. In previous animal studies, metabolic disruptions in amino acid metabolism, lipid metabolism, and the TCA cycle have been reported following exposure of morphine<sup>5</sup> and heroin<sup>5,6</sup>. Hair or blood samples obtained from individuals with a history of MA addiction or abuse have been extensively subjected to metabolic phenotyping<sup>7–9</sup>. One hurdle in treating drug use disorders is the lack of United States Food and Drug Administration-approved medications or other pharmacotherapies for psychostimulant use disorders<sup>10</sup>. Recent studies on MA use disorders have emphasized the identification of diagnostic markers and therapeutic targets. To meet this objective, metabolomic characterization of MA use disorders has garnered particular interest, with a focus on amino acid metabolism, lipid metabolism, and the TCA cycle.

Based on the theory proposed during the development of methadone maintenance programs, addiction can be considered a metabolic disease, given that it is initiated by a disruption in metabolism and causes persistent neurochemical disturbances, leading to addiction<sup>11,12</sup>. As evidence supporting metabolic disturbances in the process of developing MA use disorder, our previous study uncovered immediate and distinct changes in the metabolic pathways involved in energy metabolism, the nervous system, and membrane lipid metabolism in the plasma of MA self-administering rats during 24 h of short-term abstinence<sup>13</sup>. Wang et al. also observed metabolic disturbances in the serum of MA abusers, particularly perturbations in energy and amino acid metabolism<sup>8</sup>. Network analysis based on substantially altered metabolomes in human hair has demonstrated that heavy MA abuse affects the biosynthesis or metabolism of lipids, such as glycosphingolipids, sphingolipids, glycerophospholipids, and ether lipids, as well as the metabolism of amino acids<sup>14</sup>. However, no metabolomic studies have compared the multiple stages of MA exposure corresponding to drug reward, extinction, and reinstatement, which characterize the development of drug dependence. Reinstatement induced by drugs or drug-associated cues after a certain period of abstinence is a critical step in the development of drug use disorders. Therefore, understanding the metabolic signatures during the reinstatement stage of MA use disorder could facilitate the discovery of early diagnostic biomarkers and therapeutic targets.

Self-administration is a well-established animal model based on the principle of operant conditioning, in which an animal performs a specific behavior (e.g., pressing a lever) and is rewarded with a drug. The behavior exhibited by animals in self-administration experiments is similar to that of drug addicts, and data on characterized behavior patterns such as increases and decreases in lever pressing under certain conditions are used to investigate the mechanisms of physical and psychological dependence<sup>15,16</sup>. Previous studies have used the animal self-administration model to elucidate the neurological mechanisms of drug dependence and identify potential biomarkers for drug dependence<sup>17–20</sup>. In this study, we employed a rat self-administration model involving MA self-administration, extinction, and MA-primed reinstatement to explore the initial progression of drug dependence.

Blood serves as a specimen that reflects systemic metabolic changes in animal and clinical studies, while the brain reflects neurobiological processes. Blood, along with its liquid components, plasma or serum, is one of the most extensively studied sample types in metabolomics across various diseases because it mirrors systemic pathophysiological processes and provides a “snapshot” of metabolic changes influenced by factors such as age, sex, lifestyle (e.g., exercise, smoking, diet), genotype, medication, environmental factors, and others<sup>21</sup>. Furthermore, metabolomics data in blood holds significant potential as clinical diagnostic markers due to its easy accessibility and minimally invasive sampling<sup>22,23</sup>.

In the current study, we examined and correlated metabolic alterations to elucidate the stages of drug dependence progression in an MA self-administration rat model, encompassing MA self-administration, extinction, and reinstatement. To achieve this, rat plasma was collected at specific time points, i.e., immediately after 16 days of MA self-administration, after 16 days of MA self-administration followed by 14 days of extinction, after 16 days of MA SA, and after 14 days of extinction followed by priming injection of MA for reinstatement, and subjected to metabolic characterization.

## Materials and methods

### Materials and chemicals

Formic acid, 2-aminoanthracene, and 2,3,4,5,6-pentafluorobenzoic acid were purchased from Sigma Aldrich (St. Louis, MO). The AbsoluteIDQ p180 kit used for targeted analysis was purchased from Biocrates Life Sciences AG (Innsbruck, Austria). All solvents were of high-performance liquid chromatography (HPLC) grade. All other chemicals were of reagent grade.

### Animals

Male Sprague-Dawley rats (Daehan Animal, Seoul, Republic of Korea), 7 weeks old (weighing 260–280 g) at the start of the study, were housed individually in cages in the laboratory animal facility under controlled temperature ( $22 \pm 2$  °C) and humidity ( $60 \pm 2\%$ ) and with a 12 h light/dark cycle. Animals had *ad libitum* access to food and water. All experimental procedures were approved by the Institutional Animal Care and Use Committee of the Korea Institute of Toxicology, Daejeon, Republic of Korea (No. KIT-1802-0074). All methods involving animals are reported in accordance with ARRIVE guidelines. Euthanasia was done at the end of the study using carbon dioxide in accordance with the scientific research guidelines and regulations of the Korea Institute of Toxicology.

## Animal behavior study

The procedures used for food training, surgical implantation of the jugular catheter, self-administration of MA or saline (SAL), extinction training, and MA-priming-induced reinstatement were conducted as described previously<sup>24,25</sup>, with minor modifications. Rats were anesthetized with pentobarbital (50 mg/kg, intraperitoneal) and an intravenous catheter was inserted into the right jugular vein that exited the body on the dorsal surface of the scapulae. Each rat was administered Ketoprofen (0.5 mL/kg, subcutaneous) as a post-operative analgesic immediately following surgery and allowed to recover for 5 days prior to the beginning of behavioral testing<sup>13,26</sup>. Figure 1A illustrates the timeline of the animal behavior study, experimental sessions, and treatment groups. After passing the food pellet test, 34 rats underwent consecutive experimental sessions involving drug self-administration, extinction, and reinstatement in the same operating chamber. Rats were subjected to predetermined experimental sessions and classified accordingly. After a 5-day recovery period from chronic indwelling jugular catheter implantation surgery, 10 and 24 rats were exposed to self-administered SAL (Group S) and MA (0.05 mg/kg/infusion; Group M), respectively, under a fixed-ratio 1 (FR-1) 20-s time-out reinforcement schedule for 2 h/day for 16 days. Immediately after the last self-administration session, four (Group S) and six (Group M) of the 10 and 24 rats, respectively, were sacrificed for plasma collection; the remaining 6 and 18 rats were used to continue extinction to diminish the previously learned drug-seeking behavior of MA self-administered rats for 14 days (Group SS and Group MS, respectively), following the same protocol as SAL self-administration. Immediately after the last extinction session, 6 (Group SS) and 6 (Group MS) were selected for plasma collection. The remaining 12 rats, which had undergone MA self-administration and extinction, were subjected to the reinstatement session. The day after the last extinction session, the rats were intraperitoneally administered SAL (Group MSS,  $n=6$ ) or MA (0.3 mg/kg; Group MSM,  $n=6$ ) and then immediately transferred to the operant chamber for 2 h to measure the number of MA infusions and active lever presses to determine MA-seeking behavior. At the final stage, one rat each from Groups M and MSS that failed to acquire a stable response (less than 20% variation) to the lever press during the last 3 days was excluded from further experiments, with another rat in Group MS excluded due to with an insufficient sample size. The number of rats in each group was as follows: Group S,  $n=4$ ; Group M,  $n=5$ ; Group SS,  $n=6$ ; Group MS,  $n=5$ ; Group MSS,  $n=5$ ; and Group MSM,  $n=6$  (Fig. 1A).

## Plasma sampling

Rats were anesthetized with pentobarbital (50 mg/kg, intraperitoneal) and sacrificed to obtain blood samples. Blood was collected through the abdominal vena cava (approximately 5 mL), and aliquots were transferred to EDTA tubes (BD Vacutainer® K2E (EDTA) 18.0 mg, BD Biosciences, Franklin Lakes, NJ, USA). After a brief mixing period, the tubes were allowed to stand at room temperature for 30 min. Following centrifugation at 1624 $\times g$  for 10 min at 4 °C, the supernatant (plasma) was transferred to a 1.5 mL microfuge tube and stored at –80 °C before analysis<sup>13</sup>.

## Targeted and non-targeted metabolomics analysis

All sample preparation and instrumental analyses for targeted and non-targeted metabolomic analyses were conducted following the procedures outlined in our previous study<sup>13</sup>, with the exception of the analysis of tricarboxylic acid (TCA) metabolites, which were investigated using our validated in-house method. For targeted metabolomic analysis of 40 acylcarnitines, 42 amino acids and biogenic amines, 90 glycerophospholipids, 15 sphingolipids, and 1 monosaccharide, samples were prepared using the AbsoluteIDQ p180 kit (Biocrates Life Sciences AG) according to the manufacturer's instructions and analyzed using flow injection analysis (FIA)-tandem mass spectrometry (MS/MS) and HPLC-MS/MS (AB Sciex 4000 QTrap mass spectrometer, Sciex, Framingham, MA, USA). The kit was validated using MetValTM (Biocrates Life Sciences AG) software, and the analytical results were processed using AnalystTM (Sciex) and MetValTM software.

For analyzing 10 TCA metabolites, rat plasma samples were protein-precipitated using ice-cold acetone and then centrifuged at 19,274 $\times g$  for 10 min at 4 °C. The supernatants were filtered using a 0.45 μm polyvinylidenefluoride microporous membrane and filtered sample was analyzed by HPLC-MS/MS. LC-MS/MS analysis was conducted using a reverse-phase column coupled with a 1260 Infinity LC system and 6460 Triple Quadrupole MS/MS (Agilent Technologies, Santa Clara, CA, USA). Data were processed using MassHunter software (B. 08. 00; Agilent Technologies).

For non-targeted metabolomic analysis, samples were prepared by protein precipitation using acetonitrile and ultra-high-performance liquid chromatography coupled with quadrupole time-of-flight electrospray ionization (ESI) mass spectrometry (UPLC-QTOF-ESI-MS) was conducted in both positive and negative ionization modes. Analyses were performed using an Agilent 6530 Accurate-Mass Q-TOF LC/MS System with an Agilent 1290 Infinity LC (Agilent Technologies, Palo Alto, CA, USA). Pooled quality control samples, prepared by mixing aliquots from each sample, were analyzed every six sample analyses. Triplicate samples were analyzed for both targeted and non-targeted metabolomics.

## Data processing and statistical analysis

Considering the UPLC-QTOF-ESI-MS data, data processing and statistical analyses were performed using MassHunter Profinder (version 10.0) and Mass Profiler Professional (MPP, version B.15.1) software

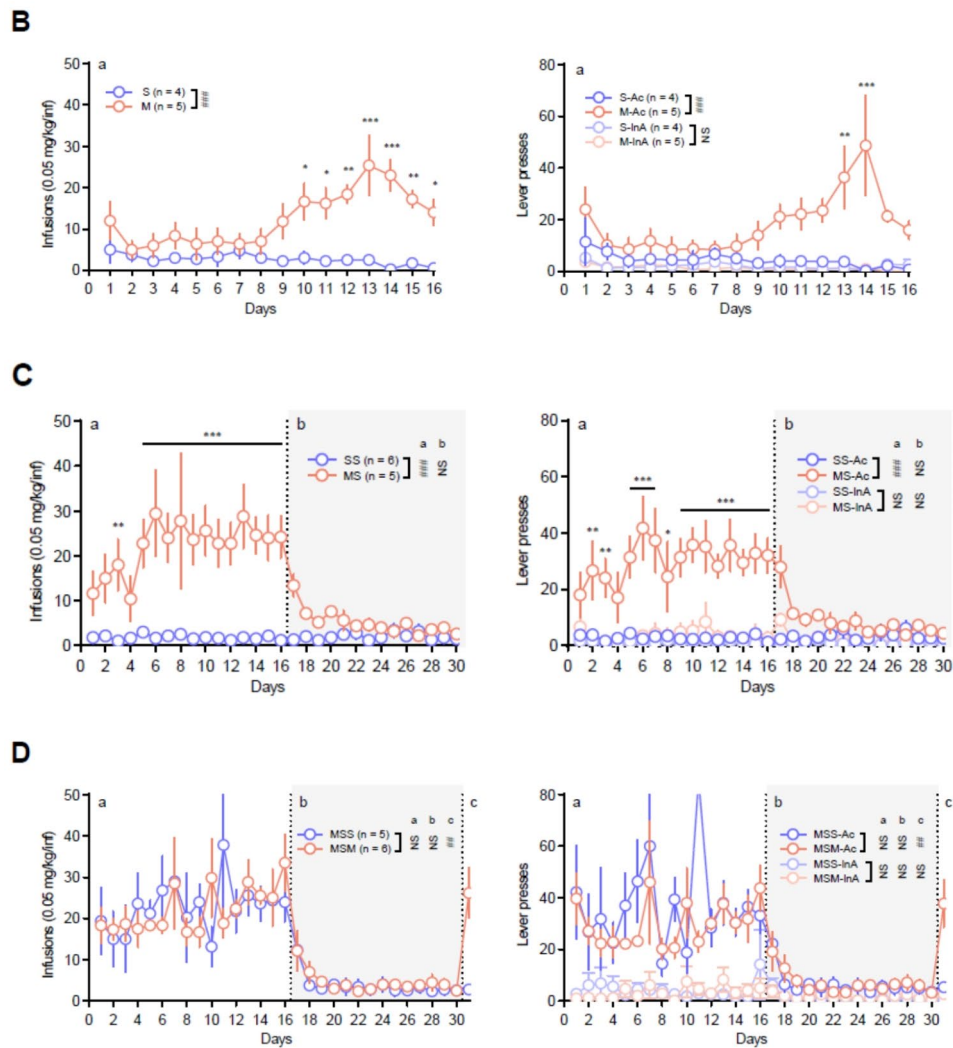
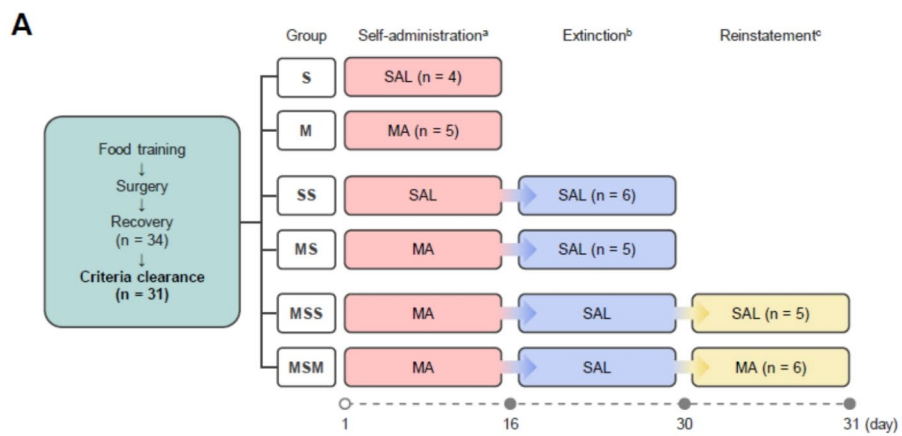


**Fig. 1.** Summary of animal behavior experiments. **(A)** Timeline, experimental sessions, and animal groups for behavioral assessment. Gray circle represents the day of blood collection. **(B)** Numbers of infusions and lever presses during the self-administration period (1–16 days) of Groups S and M. **(C)** Numbers of infusions and lever presses during self-administration (1–16 days) and extinction period (17–30 days) of Groups SS and MS. **(D)** Numbers of infusions and lever presses during self-administration (1–16 days), extinction (17–30 days), and reinstatement period (31 day) of Groups MSS and MSM. Statistical analyses were performed using the two-way ANOVA test, followed by Bonferroni's multiple comparison post hoc test. The data are presented as mean  $\pm$  standard error of the mean (SEM). \* $p$  < 0.05, \*\* $p$  < 0.01, \*\*\* $p$  < 0.001 for daily comparison between groups; # $p$  < 0.01, ## $p$  < 0.001 for total comparison between groups. NS, not significant; SAL, saline; MA, methamphetamine; Ac, active lever; InA, inactive lever.

(Agilent Technologies) as described in our previous study<sup>13</sup>, with minor modifications. The parameters for feature extraction in Profinders were as follows: peak height > 300 counts; ion species,  $[M + H]^+$  and  $[M + Na]^+$ , for positive ions, and  $[M - H]^-$  for negative ions; isotope peak spacing tolerance, 0.0025 m/z and 7.0 ppm; and charge state, a maximum of 1. Ion features were aligned and extracted based on particular masses (mass window of 10 ppm + 2.00 mDa) and retention times (retention time window of 0.5 min). The peak abundances of internal standards in the quality control and experimental samples were inspected to reduce false-negative and false-positive features. The CEF files were exported to MPP for metabolic investigation using an in-house database<sup>24</sup> and MassHunter METLIN Metabolite PCDL (Demo version, summer, 2014).

For statistical evaluation of data from both targeted and non-targeted metabolomic analyses, metabolic differences between groups were evaluated by principal component analysis (PCA) and partial least squares-discrimination analysis (PLS-DA) using the MetaboAnalyst software (version 6.0; <https://www.metaboanalyst.ca/>). The software automatically performed a model-fitting analysis of the three principal components. The data were scaled by auto scaling. A *t*-test with unequal variance, followed by multiple testing correction (Benjamini–Hochberg false discovery rate [FDR], adjusted *p*-value), was used to determine significant differences in ion features or metabolites. For targeted and non-targeted analysis data, the following criteria were applied: fold change > 1.2 with *p*-values < 0.05 among the groups. For non-targeted analysis, the data reproducibility of the significantly altered ion features were examined in the quality control samples and those with relative standard deviation (RSD) less than 20% were finally selected. Pathway analysis was also performed using the MetaboAnalyst 6.0 software.

## Results

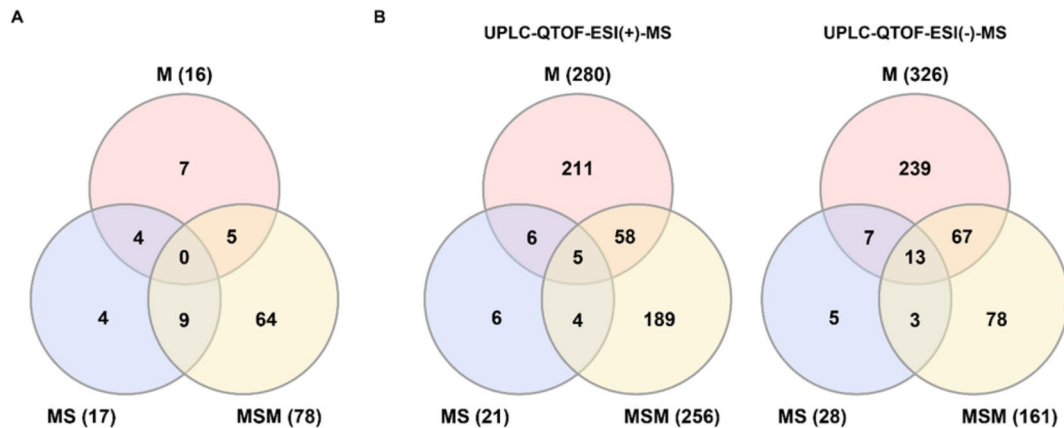
### MA self-administration, extinction, and reinstatement

Figure 1B–D present the number of infusions and lever presses during the self-administration period of Groups S and M; the self-administration and extinction periods of Groups SS and MS; and the self-administration, extinction, and reinstatement periods of Groups MSS and MSM. During the first 16 days of the self-administration session, Groups M ( $F_{1,112} = 83.27, p < 0.0001$ ) and MS ( $F_{1,144} = 180.5, p < 0.0001$ ) had a significantly higher number of drug infusions than the control groups, Groups S and SS, respectively, and showed < 20% variation during the last 3 days (Days 14–16) of the experiment. Moreover, Groups M ( $F_{1,112} = 41.45, p < 0.0001$ ) and MS ( $F_{1,143} = 209.3, p < 0.0001$ ) exhibited higher responses to the number of active levers than rats in Groups S and SS, respectively, with no significant differences observed in the number of inactive levers. Next, extinction training began the day after self-administration session. When MA access was removed, Group MS, MSS, and MSM initially maintained active lever pressing compared to Group SS on day 17 ( $p < 0.05$ ), however this behavior gradually extinguished over time. In contrast, Group SS maintained relatively low level of lever pressing behavior. Considering the extinction session, there was no significant difference in the number of drug infusions during Days 18–30 following self-administration between rats in Groups MS and MSM and those in groups SS and MSS ( $p > 0.05$ ). Additionally, there were no significant differences in the number of active and inactive levers between groups ( $p > 0.05$ ). For drug-induced reinstatement, MA and SAL (control) were administered on the day after the last extinction session. Group MSM had a significantly higher number of drug infusions and active lever presses than Group MSS ( $p < 0.01$ ). On Day 31, rats in Groups MSM and MSS performed  $26.2 \pm 2.8$  and  $2.8 \pm 1.5$  infusions (mean  $\pm$  SEM), respectively.

## Metabolomics

### Targeted analysis

Targeted metabolomics analysis was performed using a commercial analytical tool for the simultaneous quantification of 180 metabolites, 137 of which were quantified. Furthermore, our quantitative method was used to determine 10 TCA metabolites (Table S1). Data from the MA exposure groups were compared with those from the corresponding age-matched control groups (Group S vs. M, SS vs. MS or MSM). Performing the *t*-test between groups resulted in the selection of 16, 17, and 78 metabolites that were significantly altered based on the drug dependence stages (Fig. 2A). The PCA score plots revealed the most significant separation between Groups S and M (described by 40.1% of PC1), followed by the separation between Groups SS and MSM (described by 47.5% of PC1), and between Groups SS and MS (described by 40.7% of PC1) (Fig. S1A). According to the PLS-DA score plots, Groups M/MS/MSM were clearly separated from each control group, with  $Q^2$  values of 0.95, 0.80, and 0.87, and  $R^2$  values of 0.98, 0.91, and 0.95, respectively, indicating the reliability of the models (Fig. S1B). Volcano plots show statistically significant up- or downregulated metabolites in each group ( $p < 0.05$ , fold change > 1.2). In Group M, eight metabolites each were upregulated and downregulated, respectively. Group MS exhibited 17 downregulated metabolites, whereas Group MSM had 78 downregulated metabolites (Fig. S1C). As illustrated in Fig. 3, the results of the targeted analysis revealed the levels of 93 significantly altered metabolites (1 acylcarnitine, 10 amino acids and biogenic amines, 68 glycerophospholipids, 6 sphingolipids, and 8 TCA metabolites) during at least in one stage. The significance test demonstrated that the levels of these metabolites were significantly altered to different degrees depending on the type of metabolite and drug dependence stages. Among the nine quantified carnitines, only acetylcarnitine was significantly upregulated in Group M. The levels of three polyamines (putrescine, spermidine, and spermine) that were significantly increased in Group M were restored to normal concentrations or decreased below the initial levels in Group MS and/or MSM. The concentrations of methionine and proline were reduced in Group M, whereas those of citrulline, ornithine, and threonine were reduced in Group MSM. No significant changes were observed in the other groups. Most glycerophospholipids (81 of 90 metabolites) and sphingolipids (all 15 metabolites) were quantified in the rat plasma samples. Sixty-eight glycerophospholipids, including lysophosphatidylcholines (lysoPCs) and phosphatidylcholines (PCs),



**Fig. 2.** Venn diagrams of the numbers of significantly altered metabolites or ion features. (A) Targeted analysis. (B) Non-targeted analysis.

were significantly downregulated during one or two stages of drug dependence, with no upregulation detected. Notably, 62 glycerophospholipids were downregulated in Group MSM. Five sphingomyelins (SMs) (SM (OH) C14:1, SM (OH) C22:2, SM C16:1, SM C18:1, and SM C24:0) were significantly downregulated in Group MSM, with no significant alterations observed in the other groups. The levels of SM C18:0 fluctuated across each stage, showing a significant increase in Group M, a decrease in Group MS, and no significant change in Group MSM. The concentrations of major TCA metabolites, including citric acid, 2-hydroxyglutaric acid, isocitric acid, lactic acid, malic acid, pyruvic acid, succinic acid, and alpha-ketoglutaric acid, were altered significantly. Specifically, lactic acid, pyruvic acid, and alpha-ketoglutaric acid were upregulated in Group M, whereas lactic acid, pyruvic acid, and succinic acid were downregulated in Group MS. In Group MSM, citric acid, 2-hydroxyglutaric acid, isocitric acid, malic acid, and succinic acid were downregulated.

#### Non-targeted analysis

In accordance with the criteria outlined in “[Data processing and statistical analysis](#)”, the aligned ion features in each experimental sample were extracted from the UPLC-QTOF-ESI-MS data in both positive and negative ionization modes. Data processing and statistical analyses were further performed for differential and significance analyses. As shown in Fig. 2B, 21 and 280, 21, and 256 significantly altered ion features from the positive ESI analysis were obtained in the plasma samples of Groups M, MS, and MSM, respectively, compared with the respective control groups ( $p < 0.05$ , fold change  $> 1.2$ ). Based on the negative ESI analysis, we detected 326, 28, and 161 significantly altered ion features ( $p < 0.05$ , fold change  $> 1.2$ ). The PCA score plots demonstrated a clear separation between Groups S and M, described by 25.5 and 25% of PC1 in each positive and negative ESI mode, respectively, while a large overlap was observed between Groups SS and MS or MSM (Fig. S2A). The 10-fold cross-validation results using the PLS-DA model revealed that Groups M/MS/MSM were notably discriminated from each control group in both the positive ( $Q^2$ , 0.99/0.86/0.96;  $R^2$ , 1.0/0.99/0.99) and negative ESI modes ( $Q^2$ , 0.99/0.80/0.95;  $R^2$ , 1.0/0.97/0.99) (Fig. S2B). Volcano plots depicted ion features, the levels of which were significantly increased or decreased in each group in positive and negative ESI modes (Fig. S2C). Table 1 lists the metabolites identified in rat plasma with an 80% frequency among all analyzed samples using an in-house database<sup>24</sup>. Metabolites exhibiting significant changes and associated fold changes are indicated. Group M showed significantly elevated levels of sphinganine, N-acetyl-l-phenylalanine, linolenic acid, 4-methyl-2-oxo-pentanoic acid, and 4-pyridoxate, along with significantly reduced levels of norvaline, thyroxine, cholate, glycocholate, hippurate, and uridine. Hippurate and N-acetyl-l-phenylalanine were downregulated significantly in Group MS. In Group MSM, hippurate was downregulated, whereas linolenic acid was upregulated.

#### Metabolic pathway analysis

Metabolic pathway analysis was performed to better understand the alterations in metabolite levels based on the progression of MA-dependence. The three circles located at the top right of Fig. 4A ( $p < 0.05$ , impact  $> 0.2$ ) and Table 2 show the significantly altered metabolic pathways: the citrate cycle (TCA cycle), arginine and proline metabolism, and arginine biosynthesis. These metabolic pathways were mutually affected and dynamically changed during drug dependence progression in MA self-administered rats, as shown in Fig. 4B, produced by the integration of targeted and non-targeted metabolomics data. Interestingly, the pathways of the biosynthesis and metabolism of arginine, proline, and citrate cycles were upregulated in Group M and recovered in Group MS. However, these pathways were notably downregulated in the MSM group.

#### Discussion

Targeted and non-targeted metabolomics, integrated with bioinformatics, have previously been used to explore the effects of addictive drugs and identify potential biomarkers for the diagnosis and treatment of drug use disorders. Metabolic changes, such as drug reward, withdrawal, and reinstatement, have been predominantly studied at different stages of drug dependence progression using animal models<sup>13,27–30</sup>. However,

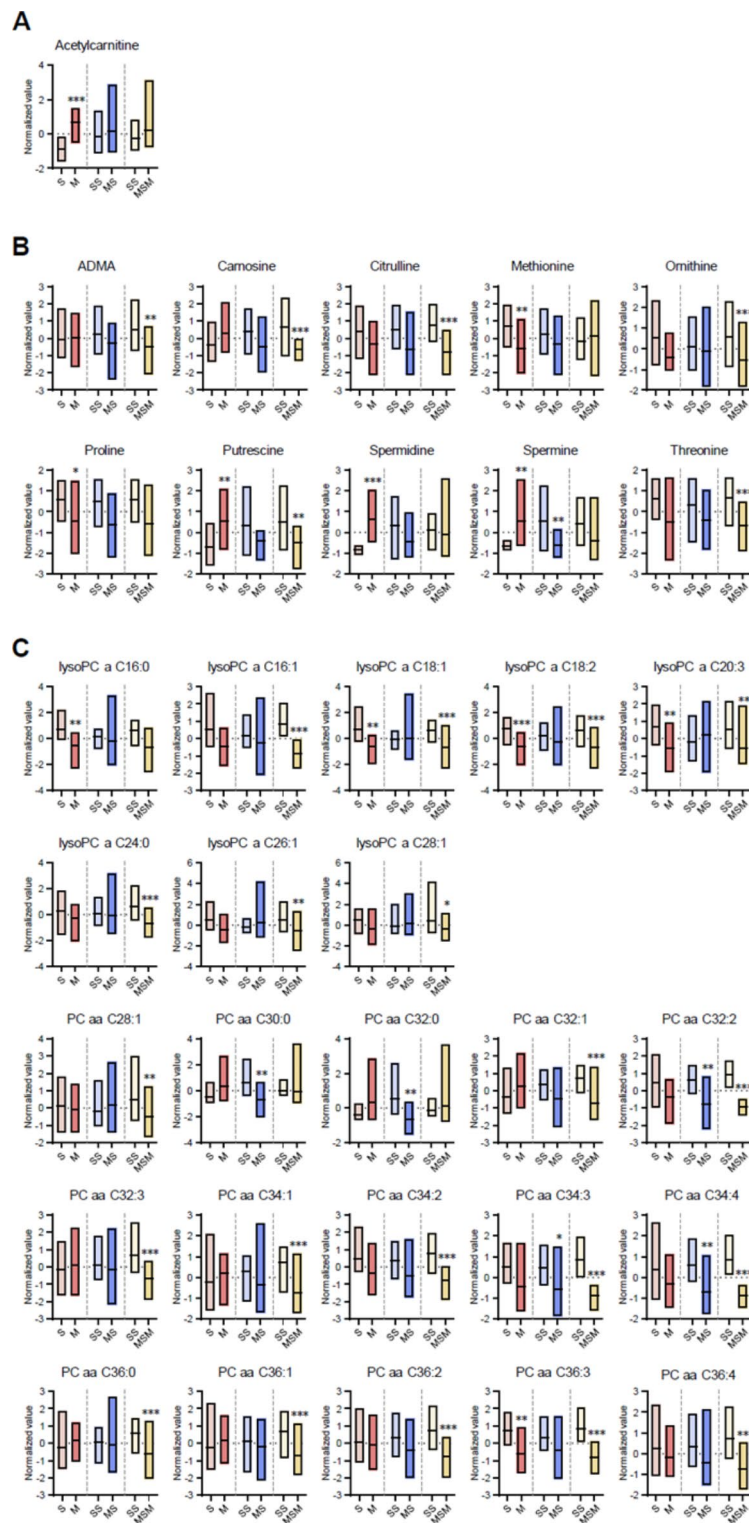


**Fig. 3.** Box plots of the target metabolites in plasma collected from methamphetamine self-administering rats at different stages of drug dependence progression. (A) Acetylcarnitine. (B) Amino acids and biogenic amines. (C) Glycerophospholipids. (D) Sphingolipids. (E) TCA intermediates. Statistical analyses were performed using the Student's *t*-test and normalized values of all the experimental groups were determined using the normalized  $\log_2$  transformed and median normalized data (fold change  $> 1.2$ ). The box plots were generated using GraphPad Prism 8.  $*p < 0.05$ ,  $**p < 0.01$ ,  $***p < 0.001$ . TCA, tricarboxylic acid.

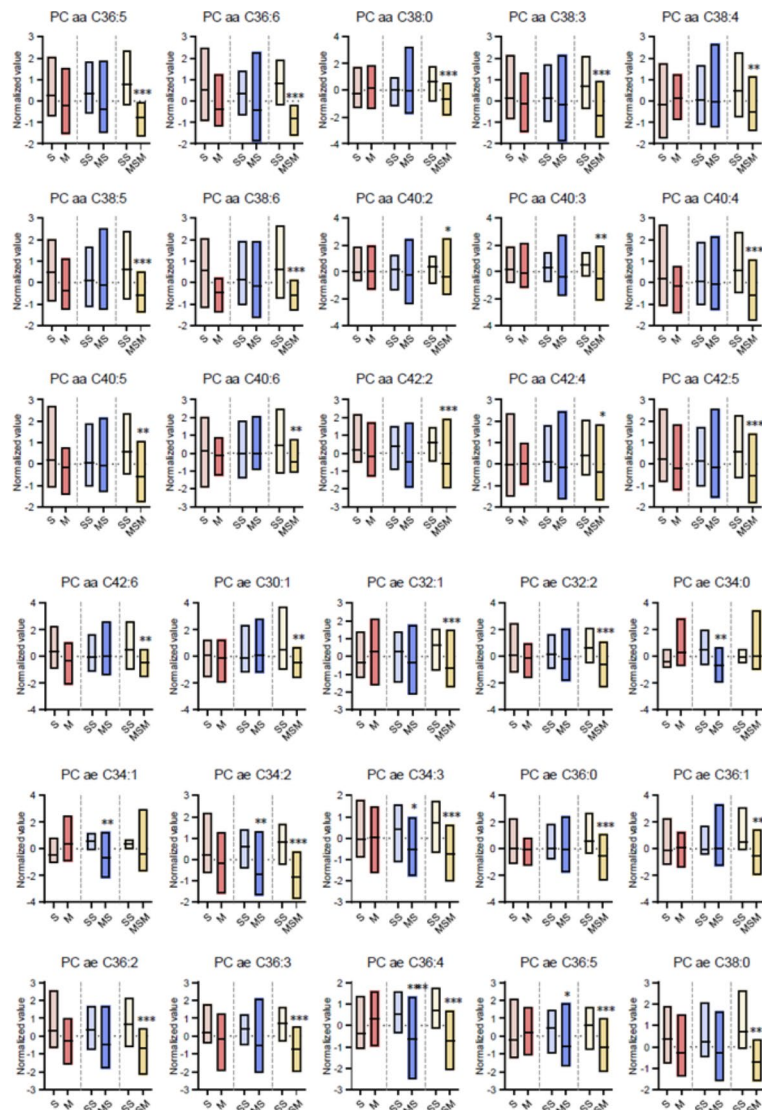


Figure 3. (continued)

to comprehensively understand drug dependence, it is crucial to investigate metabolomic alterations across multiple stages. Previous metabolomic studies have highlighted disruptions in the TCA cycle, amino acid metabolism, and lipid metabolism during drug exposure, withdrawal, and re-exposure using rodent urine and serum following intraperitoneal (i.p.) injection of morphine<sup>5</sup> and heroin<sup>5,6</sup>. Heroin administration has been found to substantially disrupt these metabolic pathways, leading to increased energy metabolism. However, during heroin withdrawal, most metabolites return to baseline levels with only a few exceptions<sup>6</sup>. However, there is a limitation in the literature regarding metabolic characterization during the progression of MA dependence. In the current study, we performed an integrated investigation of targeted and non-targeted metabolomics in plasma collected at various time points after MA self-administration, subsequent extinction, and reinstatement with a priming injection of MA to elucidate the dynamic metabolic changes associated with the progression of drug dependence.

The high rate of relapse triggered by various stimuli such as stress, contextual cues, and reminders of past drug use plays a critical role in inducing drug dependence<sup>31</sup>. Previous studies have investigated drug relapse behaviors by observing cue-induced<sup>32</sup>, context-induced<sup>33</sup>, stress-induced<sup>34</sup>, and drug-primed reinstatement<sup>35,36</sup> in animal models of drug self-administration to simulate clinical scenarios. Animal models of drug self-administration, known for their strong validity in depicting drug intake and abuse, are considered standard models for elucidating human addiction behaviors<sup>37</sup>. In the current study, we used a rat self-administration model with 2 h/day access to the drug to elucidate the initial vulnerability to drug dependence. This model features comparatively short training sessions and reliable induction of extinction and relapse behaviors. The drug-dependent stages of MA self-administration, extinction, and reinstatement were carefully constructed, and metabolic alterations were studied within this framework.

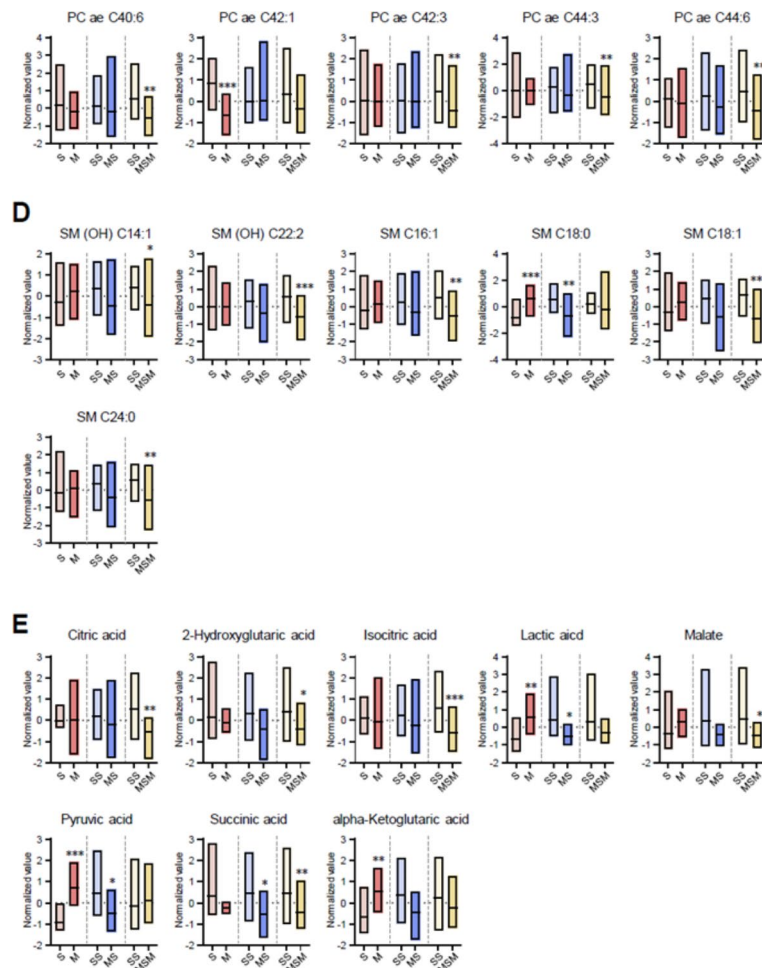
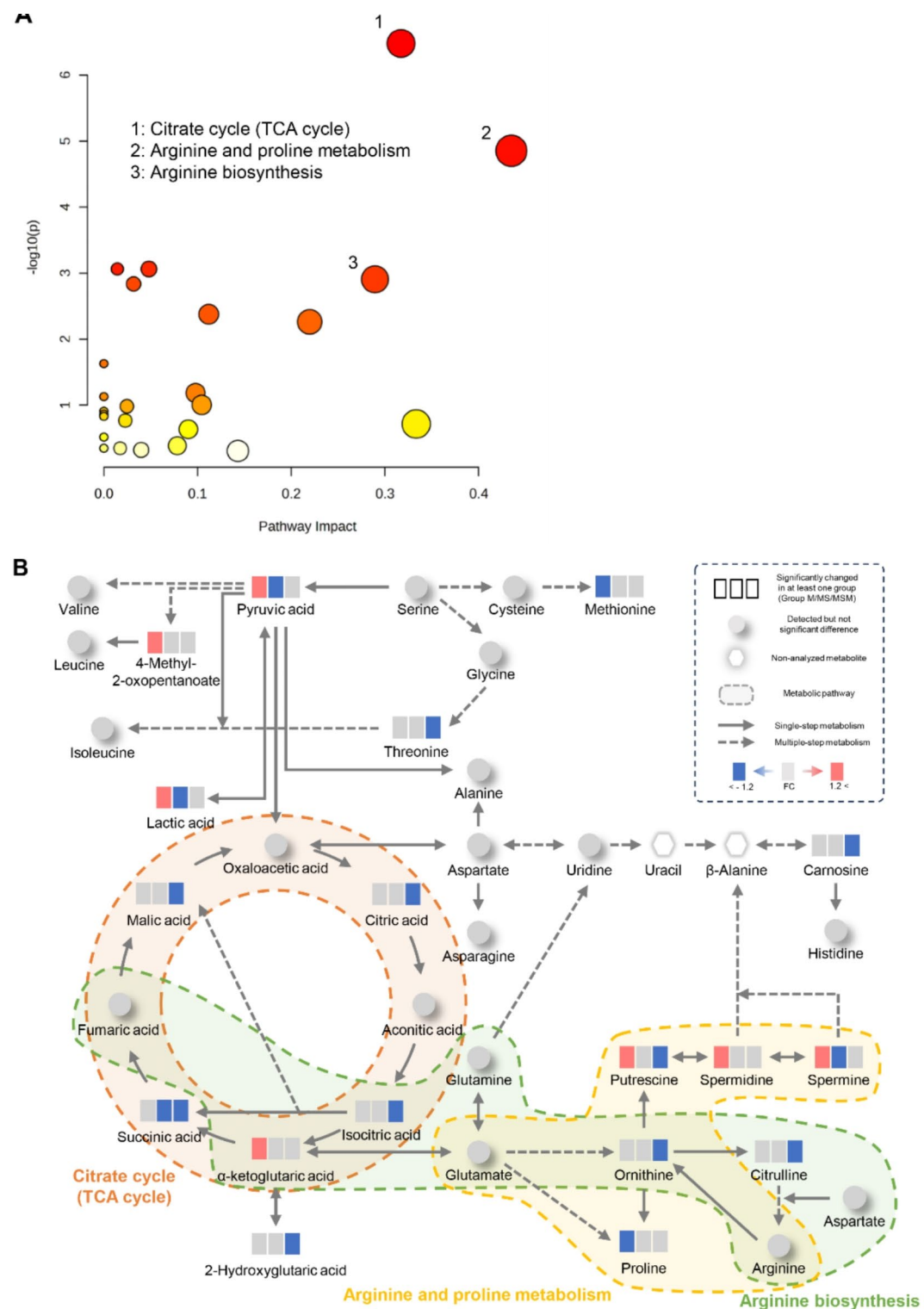


Figure 3. (continued)

Ionization polarity	m/z	t <sub>r</sub> (min)	Δt <sub>r</sub> (min)	Formular	Mass	Δmass (ppm)	Metabolite (Fold change)	Ion species	Score
Positive	180.0651	6.872	-0.285	C <sub>9</sub> H <sub>9</sub> NO <sub>3</sub>	179.0580	-1.14	Hippurate (#-1.68, †-1.85)	(M+H)+	73.79
	118.0859	1.051	0.092	C <sub>5</sub> H <sub>11</sub> NO <sub>2</sub>	117.0786	-3.20	Norvaline (*-1.45)	(M+H)+	87.02
	302.3046	35.953	-0.002	C <sub>18</sub> H <sub>39</sub> NO <sub>2</sub>	301.2972	-2.79	Sphinganine (*1.56)	(M+H)+	88.79
	777.6930	34.079	-0.066	C <sub>15</sub> H <sub>11</sub> I <sub>4</sub> NO <sub>4</sub>	776.6854	-1.60	Thyroxine (*-1.51)	(M+H)+	93.92
Negative	206.0818	12.954	-0.464	C <sub>11</sub> H <sub>13</sub> NO <sub>3</sub>	207.0889	-2.89	N-acetyl-l-phenylalanine (*2.10, #-1.96)	(M-H)-	57.16
	407.2802	35.205	0.001	C <sub>24</sub> H <sub>40</sub> O <sub>5</sub>	408.2873	-0.57	Cholate (*-2.41)	(M-H)-	99.00
	437.2903	36.379	-0.100	C <sub>21</sub> H <sub>40</sub> O <sub>4</sub>	392.2920	-1.78	Deoxycholate	(M+HCOO)-	93.89
	464.3015	34.376	0.001	C <sub>26</sub> H <sub>43</sub> NO <sub>6</sub>	465.3086	-0.91	Glycocholate (*-2.97)	(M-H)-	99.09
	178.0507	6.869	-0.288	C <sub>9</sub> H <sub>9</sub> NO <sub>3</sub>	179.0580	-1.55	Hippurate (*-1.51)	(M-H)-	67.38
	277.2165	38.504	-0.238	C <sub>18</sub> H <sub>30</sub> O <sub>2</sub>	278.2238	-2.92	alpha-Linolenic acid (*1.60, †1.67)	(M-H)-	79.02
	129.0557	4.176	-0.076	C <sub>6</sub> H <sub>10</sub> O <sub>3</sub>	130.0630	-0.16	4-Methyl-2-oxo-pentanoic acid (*2.57)	(M-H)-	88.86
	182.0457	2.984	-0.311	C <sub>8</sub> H <sub>9</sub> NO <sub>4</sub>	183.0530	-0.93	4-Pyridoxate (*2.05)	(M-H)-	74.45
	203.0822	4.054	-0.261	C <sub>11</sub> H <sub>12</sub> N <sub>2</sub> O <sub>2</sub>	204.0895	-2.10	Tryptophan	(M-H)-	77.73
	243.0615	1.667	-0.083	C <sub>9</sub> H <sub>12</sub> N <sub>2</sub> O <sub>6</sub>	244.0689	-2.45	Uridine (*-1.97)	(M-H)-	84.18

**Table 1.** Metabolites identified in rat plasma via UPLC-QTOF-ESI-MS analysis and in-house database matching.  $p < 0.05$ , for at least one condition (\*Group M, #Group MS, †Group MSM) versus each control group. Fold changes are indicated in parentheses.



**Fig. 4.** Results of metabolic pathway analysis. (A) Metabolic pathway analysis using MetaboAnalyst. The size and color of each circle represent pathway impact value and p-value, respectively. (B) Alterations in metabolic pathways depending on methamphetamine (MA) dependence progression. Down- and upregulated metabolites are highlighted in blue and red, respectively. Gray color represents no significant change. The colored portions inside the dotted line are significant metabolic pathways. The solid and dotted line arrows represent single-step and multiple-step metabolic pathways between metabolites. TCA, tricarboxylic acid.

No.	Metabolic pathway	Total	p-value	Impact	Hit	Metabolites
1	Citrate cycle (TCA cycle)	20	0.000	0.3	6	Citric acid, isocitric acid, alpha-ketoglutaric acid, malic acid, pyruvic acid, and succinic acid
2	Arginine and proline metabolism	36	0.001	0.4	6	Ornithine, proline, putrescine, pyruvic acid, spermidine, and spermine
3	Arginine biosynthesis	14	0.019	0.3	3	Citrulline, alpha-ketoglutaric acid, and ornithine

**Table 2.** Altered metabolic pathways during drug dependence progression in methamphetamine self-administrating rats. TCA, tricarboxylic acid.

Groups M, MS, and MSM were designed considering MA rewards, withdrawal, and relapse. Interestingly, both targeted and untargeted analyses showed that Group MSM exhibited notable metabolic changes, distinct from Groups M and MS (Fig. 2). Based on animal and clinical observations, understanding cue-induced drug cravings after withdrawal holds substantial potential for diagnosing and treating drug addiction<sup>25,38,39</sup>. In a previous study, transcriptomic profiling of brain regions involved in the brain's reward circuitry (prefrontal cortex, dorsal striatum, nucleus accumbens, basolateral amygdala, ventral hippocampus, and ventral tegmental area) revealed considerable changes in transcript expression during the cocaine self-administration, withdrawal, and relapse phases, with the greatest changes detected in the re-exposure phase<sup>40</sup>. Our metabolomic data from sequentially designed animal experiments support the concept that novel potential diagnostic or treatment targets for drug dependence should focus on drug reinstatement.

MA self-administration, followed by extinction and priming injection of MA, impacted several targeted functional metabolites of acylcarnitines, amino acids and biogenic amines, glycerophospholipids, and sphingolipids. In particular, the degree of metabolite variation differed between Groups M and MSM despite the same immediate sampling time following MA self-administration. Glycerophospholipid levels were considerably affected during relapse.

The toxicity of MA is characterized by a decrease in monoamine synthesis and disruption of synaptic integrity<sup>41</sup>, accompanied by neuronal degeneration and cell death<sup>42</sup>. Moreover, growing evidence suggests that amphetamine and MA administration increase free radical formation and damage mitochondria, resulting in secondary excitotoxicity and failure of cellular energy metabolism<sup>43</sup>. From this perspective, the importance of carnitine, which plays a role in energy conversion by transporting long-chain fatty acyl groups to mitochondria for  $\beta$ -oxidation, has been revealed<sup>44</sup>. The administration of acetyl-L-carnitine along with MA (increasing from 1 to 5 mg/kg, i.p.) for 10 days was shown to attenuate the severity of symptoms caused by non-use of the drug during the subsequent 10-day withdrawal period in Wistar rats<sup>45</sup>. Furthermore, acetyl-L-carnitine administration reduced MA-induced behavioral sensitization in an MA challenge performed after 7 days of MA administration at 2.5 mg/kg, followed by a 7-day withdrawal period in CD1 mice<sup>46</sup>. Previous studies using cell lines have reported the preventive effects of acetyl-L-carnitine against structural damage caused by MA-induced toxicity<sup>47,48</sup>. In our study, elevated acetylcarnitine levels during the MA reward stage implies a homeostatic response to restore the balance of energy metabolism or neuronal function disturbed by MA exposure.

Several animal studies have explored the metabolic profiles of amino acids and polyamines following addictive drug administration and withdrawal; however, there have been no studies on relapse-induced metabolic perturbations. Reportedly, serum and urine levels of citrulline, ornithine, threonine, and methionine were found decrease substantially following both single (10 mg/kg, i.p.) and escalating (10, 12.5, 15, 20, and 30 mg/kg, i.p.) administration of MA, returning to baseline levels after a 2-day withdrawal period in Sprague Dawley rats<sup>49</sup>. The relevance of polyamines in the development of ethanol or cocaine dependence, withdrawal-related behaviors, and neuropathological sequelae has been reported<sup>50–53</sup>. Putrescine acts as an antagonist, whereas spermidine and spermine act as agonists, regulating the activity of N-methyl-d-aspartate (NMDA)-type glutamate receptors<sup>50</sup>. The action of spermidine and spermine on NMDA receptors in alcohol and/or cocaine use disorders has been highlighted<sup>53</sup>. Additionally, repeated cocaine administration for six days (50 mg/kg, i.p.) increased putrescine levels in six brain regions, including the striatum, hippocampus, and cortex, which returned to normal levels after three days of withdrawal<sup>51</sup>. Polyamines, particularly spermine and spermidine, reportedly modulate synaptic plasticity and neurotransmission<sup>54,55</sup>. The normalization or reduction of elevated levels of three polyamines (putrescine, spermidine, and spermine) in Group MS and/or MSM following a significant increase in Group M could potentially alter the neurochemical environment, which, in turn, enhances the rewarding effects of MA and influences addiction-related processes.

The neuroprotective role of SMs in the development of drug dependence induced by psychoactive drugs, including MA, cocaine, alcohol, and morphine, has been established, suggesting their potential as therapeutic targets<sup>56</sup>. The authors of previous studies have offered insights into the dynamic alterations of different lipid species due to psychostimulant exposure and their strong connection with lipid metabolic enzymes, such as sphingomyelin phosphodiesterase (SMase) and phospholipase A2 (PLA2). This was achieved through brain lipid profiling in a cocaine-conditioned place preference model<sup>57</sup> and after seven days of repeated administration of MA (3 mg/kg, i.p.) in C57BL/6 mice<sup>58</sup>. Moreover, a decrease in phosphocholine cytidylyltransferase and PLA2 expression has been documented in the postmortem brains of individuals who abused cocaine and MA<sup>59</sup>, and reduced levels of PLA2 have been observed in the brains of rats subjected to chronic cocaine administration<sup>60</sup>. The distinct downregulation of glycerophospholipids and SMs in Group MSM implied that these lipids could be crucial regulators of MA reinstatement.

Exposure to MA has been shown to disrupt energy metabolism by affecting mitochondrial function and interfering with the utilization of key metabolites, such as pyruvic and lactic acid, for energy production<sup>49,61</sup>. In the current study, we detected the upregulation of pyruvic acid and lactic acid in Group M, followed by

downregulation in Group MS. This pattern aligns with the findings from studies on NMRI mice (3 mg/kg, subcutaneous)<sup>62</sup> and Sprague Dawley rats (10×3 and 5 mg/kg, i.p.) exposed to MA<sup>63</sup>, in which changes in these metabolites were linked to altered energy metabolism. Furthermore, several TCA intermediates, including citric acid, 2-hydroxyglutaric acid, isocitric acid, malic acid, and succinic acid, were downregulated in Group MSM without any upregulation. Similar MA-induced disturbances in TCA metabolism have been reported previously despite differences in dosage and administration methods. In Sprague Dawley rats administered MA (10 mg/kg × 4, i.p.), significantly downregulated levels of various TCA intermediates, including α-ketoglutaric acid, malic acid, succinic acid, citric acid, isocitric acid, and pyruvic acid, were found to return to baseline levels after 72 h<sup>64</sup>. Moreover, reduced levels of methionine and TCA intermediates were observed in the brains of Wistar rats treated with 2.5 mg/kg MA twice daily for a week<sup>65</sup>. Additionally, metabolic changes in the serum of MA abusers showed decreased levels of threonine, proline, methionine, and TCA intermediates, such as lactic acid, citric acid, pyruvic acid, and succinic acid<sup>66</sup>. The consistent downregulation of TCA intermediates following MA exposure in both the current and previous studies suggests that both initial MA exposure and subsequent re-exposure may lead to increased energy consumption.

It is important to evaluate and examine the endpoints in animal models of drug addiction, such as self-administration, to capture the unique molecular or metabolic characteristics of drug use disorders<sup>13,30,67,68</sup>. Drug self-administration can be significantly influenced by environmental conditions (e.g., feeding conditions, palatable dietary substances, stress) and individual differences (e.g., reactivity level, age, sex, dietary preferences, genetics) even under the same pharmacological conditions such as drug dose, drug history, and pretreatment drugs<sup>69</sup>. Therefore, both the targeted and non-targeted metabolomics data from the MA exposure groups were compared with those from the corresponding age-matched control groups (Group S vs. M, SS vs. MS or MSM) rather than comparing the data from Groups M, MS, and MSM with each other. Chronic drug exposure can manifest differently at the transcriptional or metabolic level, depending on whether levels were assessed during early withdrawal, late withdrawal, or the relapse phase. Our findings suggest that each phase of MA reward, withdrawal, and relapse induce specific changes in metabolic pathways, particularly those related to the TCA cycle, arginine and proline metabolism, and arginine biosynthesis. The TCA cycle plays a crucial role in energy metabolism, whereas arginine and proline metabolism, along with arginine biosynthesis, are involved in neurotransmitter action through nitric oxide (NO)<sup>70–72</sup>, synaptic plasticity<sup>73,74</sup>, and stress responses<sup>75,76</sup>, affecting various aspects of brain function. Abnormalities in these functions contribute to drug addiction and increase vulnerability to relapse<sup>77–80</sup>. These changes could represent repeated metabolic perturbations that may lead to a pathological state of MA addiction following ongoing cycles of drug reward, withdrawal, and reinstatement. Given that vulnerability to the rewarding effects of stimulants in females, i.e., sex differences in MA self-administration and relapse, have been reported in both animal and clinical studies<sup>81–85</sup>, further research is necessary to compare metabolic changes between male and female models.

Although our study effectively tracked metabolic shifts associated with MA dependence, two main limitations should be addressed. First, although we followed a commonly used drug self-administration scheme, we proposed the use of an extended-access self-administration model to gain a more comprehensive understanding of drug addiction. Previous studies have combined short-access models (2 h) and long-access models (more than 6 h)<sup>86–88</sup> or adjusted the FR schedule<sup>89</sup> to better simulate the drug intake or seeking behaviors observed in humans. For instance, in a study involving cocaine and heroin, the FR-1 schedule was employed, with heroin administration adjusted to maintain the final concentration while extending the administration period by limiting the dose and number of infusions<sup>90</sup>. Although our animal model may fail to fully replicate the complex factors contributing to drug dependence in humans, it is deemed sufficiently robust to investigate relapse behavior upon re-exposure to MA. Second, despite the successful quantification and identification of metabolites through targeted and non-targeted analyses, there are limitations related to metabolomic approaches, such as coverage gaps. Targeted analyses focusing on a limited set of metabolites present challenges in capturing the full spectrum of the metabolome. Including metabolites related to neurotransmitters in the brain to monitor neurochemical changes associated with MA dependence or investigating oxidative stress pathways to clarify oxidative damage mechanisms linked to MA intoxication would enhance our understanding of the metabolic changes underlying MA dependence and improve metabolomic coverage. Furthermore, although non-targeted analysis revealed numerous ion features, the identification process was hindered by incomplete databases. Nevertheless, our study successfully distinguished the metabolic alterations associated with the progression of MA dependence and identified their relevant functionalities.

## Conclusion

Our findings suggest that each phase of MA self-administration, extinction, and reinstatement induces distinct changes in the metabolic pathways, particularly those related to the TCA cycle, arginine and proline metabolism, and arginine biosynthesis. Additionally, the decrease in glycerophospholipids and SMs suggests their potential involvement in MA reinstatement. These alterations may signify the progressive deterioration of these metabolic pathways, possibly contributing to drug dependence following repeated cycles of drug reward, withdrawal, and relapse. These results provide valuable insights into the metabolic changes associated with MA use at various stages, potentially facilitating the discovery of early diagnostic biomarkers and therapeutic targets for MA use disorders.

## Data availability

All data generated and/or analyzed during the current study available from the corresponding author upon reasonable request.

Received: 14 June 2024; Accepted: 16 September 2024

Published online: 29 September 2024

## References

- United Nations Office on Drugs and Crime (UNODC). *World Drug Report 2023* (United Nations, 2023).
- Nordahl, T. E., Salo, R. & Leamon, M. Neuropsychological effects of chronic methamphetamine use on neurotransmitters and cognition: A review. *J. Neuropsychiatry Clin. Neurosci.* **15**, 317–325. <https://doi.org/10.1176/jnp.15.3.317> (2003).
- Koob, G. F. & Volkow, N. D. Neurocircuitry of addiction. *Neuropsychopharmacology* **35**, 217–238. <https://doi.org/10.1038/npp.2009.110> (2010).
- Ashok, A. H., Mizuno, Y., Volkow, N. D. & Howes, O. D. Association of stimulant use with dopaminergic alterations in users of cocaine, amphetamine, or methamphetamine: A systematic review and meta-analysis. *JAMA Psychiatry* **74**, 511–519. <https://doi.org/10.1001/jamapsychiatry.2017.0135> (2017).
- Lu, W. et al. Identification of morphine and heroin-treatment in mice using metabolomics. *Metabolites* **11**<https://doi.org/10.3390/metabo11090607> (2021).
- Zheng, T. et al. Metabolic phenotype of rats exposed to heroin and potential markers of heroin abuse. *Drug Alcohol Depend.* **127**, 177–186. <https://doi.org/10.1016/j.drugalcdep.2012.06.031> (2013).
- Seo, M. J. et al. Mass spectrometry-based metabolomics in hair from current and former patients with methamphetamine use disorder. *Arch. Pharm. Res.* **44**, 890–901. <https://doi.org/10.1007/s12272-021-01353-3> (2021).
- Wang, T. et al. Untargeted metabolomics analysis by gas chromatography/time-of-flight mass spectrometry of human serum from methamphetamine abusers. *Addict. Biol.* **26**, e13062. <https://doi.org/10.1111/adb.13062> (2021).
- Caspani, G., Sebők, V., Sultana, N., Swann, J. R. & Bailey, A. Metabolic phenotyping of opioid and psychostimulant addiction: a novel approach for biomarker discovery and biochemical understanding of the disorder. *Br. J. Pharmacol.* **179**, 1578–1606. <https://doi.org/10.1111/bph.15475> (2022).
- Siefried, K. J., Acheson, L. S., Lintzeris, N. & Ezard, N. Pharmacological treatment of methamphetamine/amphetamine dependence: A systematic review. *CNS Drugs* **34**, 337–365. <https://doi.org/10.1007/s40263-020-00711-x> (2020).
- Dole, V. P. Narcotic addiction, physical dependence and relapse. *N. Engl. J. Med.* **286**, 988–992. <https://doi.org/10.1056/nejm197205042861808> (1972).
- Kim, M. et al. Current understanding of methamphetamine-associated metabolic changes revealed by the metabolomics approach. *Metabolites* **9**<https://doi.org/10.3390/metabo9100195> (2019).
- Kim, S. et al. Integrated non-targeted and targeted metabolomics uncovers dynamic metabolic effects during short-term abstinence in methamphetamine self-administering rats. *J. Proteome Res.* **18**, 3913–3925. <https://doi.org/10.1021/acs.jproteome.9b00363> (2019).
- Kim, S. et al. Revealing metabolic perturbation following heavy methamphetamine abuse by human hair metabolomics and network analysis. *Int. J. Mol. Sci.* **21**<https://doi.org/10.3390/ijms21176041> (2020).
- Corrigall, W. A. Nicotine self-administration in animals as a dependence model. *Nicotine Tob. Res.* **1**, 11–20. <https://doi.org/10.1080/14622299050011121> (1999).
- Spanagel, R. Animal models of addiction. *Dialogues Clin. Neurosci.* **19**, 247–258. <https://doi.org/10.31887/DCNS.2017.19.3/rspanagel> (2017).
- Yanagita, T. Self-administration studies on psychological dependence. *Trends Pharmacol. Sci.* **1**, 161–164 (1979).
- Kilbey, M. M. & Ellinwood, E. H. Jr. Self-administration of morphine in the cat. *Int. J. Addict.* **15**, 447–460. <https://doi.org/10.3109/10826088009040030> (1980).
- Spano, M. S., Fadda, P., Fratta, W. & Fattore, L. Cannabinoid-opioid interactions in drug discrimination and self-administration: Effect of maternal, postnatal, adolescent and adult exposure to the drugs. *Curr. Drug Targets* **11**, 450–461. <https://doi.org/10.2174/138945010790980295> (2010).
- Wang, L., Wu, N., Zhao, T. Y. & Li, J. The potential biomarkers of drug addiction: proteomic and metabolomics challenges. *Biomarkers* **21**, 678–685. <https://doi.org/10.1080/1354750x.2016.1201530> (2016).
- MacIntyre, D. A. et al. Serum metabolome analysis by 1H-NMR reveals differences between chronic lymphocytic leukaemia molecular subgroups. *Leukemia* **24**, 788–797. <https://doi.org/10.1038/leu.2009.295> (2010).
- Breier, M. et al. Targeted metabolomics identifies reliable and stable metabolites in human serum and plasma samples. *PLoS One* **9**, e89728. <https://doi.org/10.1371/journal.pone.0089728> (2014).
- Alasmari, E. et al. Serum metabolomic analysis of male patients with cannabis or amphetamine use disorder. *Metabolites* **12**<https://doi.org/10.3390/metabo12020179> (2022).
- Choi, B. et al. Metabolic characterization in urine and hair from a rat model of methamphetamine self-administration using LC-QTOF-MS-based metabolomics. *Metabolomics* **13**, 119. <https://doi.org/10.1007/s11306-017-1257-0> (2017).
- Towers, E. B. et al. Transcriptional Profile of Exercise-Induced Protection against Relapse to Cocaine seeking in a rat model. *Biol. Psychiatry Glob Open. Sci.* **3**, 734–745. <https://doi.org/10.1016/j.bpsgos.2023.01.007> (2023).
- Davis, J. A. Mouse and rat anesthesia and analgesia. *Curr. Protoc. Neurosci.* (Appendix 4, Appendix 4B) <https://doi.org/10.1002/0471142301.nsa04bs42> (2008).
- Eipper-Mains, J. E. et al. Effects of cocaine and withdrawal on the mouse nucleus accumbens transcriptome. *Genes Brain Behav.* **12**, 21–33. <https://doi.org/10.1111/j.1601-183X.2012.00873.x> (2013).
- Krasnova, I. N. et al. CREB phosphorylation regulates striatal transcriptional responses in the self-administration model of methamphetamine addiction in the rat. *Neurobiol. Dis.* **58**, 132–143. <https://doi.org/10.1016/j.nbd.2013.05.009> (2013).
- Goodwin, C. R. et al. Phenotypic mapping of metabolic profiles using self-organizing maps of high-dimensional mass spectrometry data. *Anal. Chem.* **86**, 6563–6571. <https://doi.org/10.1021/ac5010794> (2014).
- Ning, T., Leng, C., Chen, L., Ma, B. & Gong, X. Metabolomics analysis of serum in a rat heroin self-administration model undergoing reinforcement based on (1)H-nuclear magnetic resonance spectra. *BMC Neurosci.* **19**, 4. <https://doi.org/10.1186/s12868-018-0404-5> (2018).
- Bossert, J. M., Marchant, N. J., Calu, D. J. & Shaham, Y. The reinstatement model of drug relapse: Recent neurobiological findings, emerging research topics, and translational research. *Psychopharmacol. (Berl.)* **229**, 453–476. <https://doi.org/10.1007/s00213-013-3120-y> (2013).
- Gass, J. T., Osborne, M. P., Watson, N. L., Brown, J. L. & Olive, M. F. mGluR5 antagonism attenuates methamphetamine reinforcement and prevents reinstatement of methamphetamine-seeking behavior in rats. *Neuropsychopharmacology* **34**, 820–833. <https://doi.org/10.1038/npp.2008.140> (2009).
- Bossert, J. M. & Stern, A. L. Role of ventral subiculum in context-induced reinstatement of heroin seeking in rats. *Addict. Biol.* **19**, 338–342. <https://doi.org/10.1111/adb.12015> (2014).
- Cruz, F. C., Leão, R. M., Marin, M. T. & Planeta, C. S. Stress-induced reinstatement of amphetamine-conditioned place preference and changes in tyrosine hydroxylase in the nucleus accumbens in adolescent rats. *Pharmacol. Biochem. Behav.* **96**, 160–165. <https://doi.org/10.1016/j.pbb.2010.05.001> (2010).
- Mannangatti, P., Ramamoorthy, S. & Jayanthi, L. D. Interference of norepinephrine transporter trafficking motif attenuates amphetamine-induced locomotor hyperactivity and conditioned place preference. *Neuropharmacology* **128**, 132–141. <https://doi.org/10.1016/j.neuropharm.2017.10.005> (2018).

36. Leonard, M. Z. et al. The molecular-container calabadiol-2 prevents methamphetamine-induced reinstatement in rats: A potential approach to relapse prevention? *Int. J. Neuropsychopharmacol.* **23**, 401–405. <https://doi.org/10.1093/ijnp/pyz070> (2020).
37. Lynch, W. J., Nicholson, K. L., Dance, M. E., Morgan, R. W. & Foley, P. L. Animal models of substance abuse and addiction: Implications for science, animal welfare, and society. *Comp. Med.* **60**, 177–188 (2010).
38. Ewing, S. T. et al. Low-dose polypharmacology targeting dopamine D1 and D3 receptors reduces cue-induced relapse to heroin seeking in rats. *Addict. Biol.* **26**, e12988. <https://doi.org/10.1111/adb.12988> (2021).
39. Liu, X. et al. Preventing incubation of drug craving to treat drug relapse: From bench to bedside. *Mol. Psychiatry.* **28**, 1415–1429. <https://doi.org/10.1038/s41380-023-01942-2> (2023).
40. Walker, D. M. et al. Cocaine self-administration alters transcriptome-wide responses in the brain's reward circuitry. *Biol. Psychiatry.* **84**, 867–880. <https://doi.org/10.1016/j.biopsych.2018.04.009> (2018).
41. Ramirez, S. H. et al. Methamphetamine disrupts blood-brain barrier function by induction of oxidative stress in brain endothelial cells. *J. Cereb. Blood Flow. Metab.* **29**, 1933–1945. <https://doi.org/10.1038/jcbfm.2009.112> (2009).
42. Krasnova, I. N. & Cadet, J. L. Methamphetamine toxicity and messengers of death. *Brain Res. Rev.* **60**, 379–407. <https://doi.org/10.1016/j.brainresrev.2009.03.002> (2009).
43. Virmani, A., Gaetani, F., Imam, S., Binienda, Z. & Ali, S. The protective role of L-carnitine against neurotoxicity evoked by drug of abuse, methamphetamine, could be related to mitochondrial dysfunction. *Ann. N Y Acad. Sci.* **965**, 225–232. <https://doi.org/10.1111/j.1749-6632.2002.tb04164.x> (2002).
44. Pekala, J. et al. L-carnitine—metabolic functions and meaning in humans life. *Curr. Drug Metab.* **12**, 667–678. <https://doi.org/10.2174/138920011796504536> (2011).
45. Hoefer, M. E., Voskanian, S. J., Koob, G. F. & Pulvirenti, L. Effects of terguride, ropinirole, and acetyl-L-carnitine on methamphetamine withdrawal in the rat. *Pharmacol. Biochem. Behav.* **83**, 403–409. <https://doi.org/10.1016/j.pbb.2006.02.023> (2006).
46. Coccurello, R., Caprioli, A., Ghirardi, O. & Virmani, A. Valproate and acetyl-L-carnitine prevent methamphetamine-induced behavioral sensitization in mice. *Ann. N Y Acad. Sci.* **1122**, 260–275. <https://doi.org/10.1196/annals.1403.019> (2007).
47. Fernandes, S., Salta, S. & Summavieille, T. Methamphetamine promotes  $\alpha$ -tubulin deacetylation in endothelial cells: the protective role of acetyl-L-carnitine. *Toxicol. Lett.* **234**, 131–138. <https://doi.org/10.1016/j.toxlet.2015.02.011> (2015).
48. Fernandes, S., Salta, S., Bravo, J., Silva, A. P. & Summavieille, T. Acetyl-L-carnitine prevents methamphetamine-induced structural damage on endothelial cells via ILK-related MMP-9 activity. *Mol. Neurobiol.* **53**, 408–422. <https://doi.org/10.1007/s12035-014-8973-5> (2016).
49. Zheng, T. et al. The metabolic impact of methamphetamine on the systemic metabolism of rats and potential markers of methamphetamine abuse. *Mol. Biosyst.* **10**, 1968–1977. <https://doi.org/10.1039/c4mb00158c> (2014).
50. Williams, K., Romano, C., Dichter, M. A. & Molinoff, P. B. Modulation of the NMDA receptor by polyamines. *Life Sci.* **48**, 469–498. [https://doi.org/10.1016/0024-3205\(91\)90463-1](https://doi.org/10.1016/0024-3205(91)90463-1) (1991).
51. Shimosato, K., Watanabe, S., Marley, R. J. & Saito, T. Increased polyamine levels and changes in the sensitivity to convulsions during chronic treatment with cocaine in mice. *Brain Res.* **684**, 243–247. [https://doi.org/10.1016/0006-8993\(95\)00468-6](https://doi.org/10.1016/0006-8993(95)00468-6) (1995).
52. Prendergast, M. A. & Mulholland, P. J. Glucocorticoid and polyamine interactions in the plasticity of glutamatergic synapses that contribute to ethanol-associated dependence and neuronal injury. *Addict. Biol.* **17**, 209–223. <https://doi.org/10.1111/j.1369-1600.2011.00375.x> (2012).
53. García-Marchena, N. et al. Plasma amino acid concentrations in patients with alcohol and/or cocaine use disorders and their association with psychiatric comorbidity and sex. *Biomedicines* **10**. <https://doi.org/10.3390/biomedicines10051137> (2022).
54. Sakurada, T., Onodera, K., Tadano, T. & Kisara, K. Effects of polyamines on the central nervous system. *Jpn. J. Pharmacol.* **25**, 653–661. <https://doi.org/10.1254/jjp.25.653> (1975).
55. Makletsova, M. et al. The role of polyamines in the mechanisms of cognitive impairment. *Neurochem. J.* **16**, 283–294 (2022).
56. Kalinichenko, L. S., Gulbins, E., Kornhuber, J. & Müller, C. P. The role of sphingolipids in psychoactive drug use and addiction. *J. Neural Transm. (Vienna)* **125**, 651–672. <https://doi.org/10.1007/s00702-018-1840-1> (2018).
57. Lin, Y. et al. Cocaine modifies brain lipidome in mice. *Mol. Cell. Neurosci.* **85**, 29–44. <https://doi.org/10.1016/j.mcn.2017.08.004> (2017).
58. Jiang, L. et al. Remodeling of brain lipidome in methamphetamine-sensitized mice. *Toxicol. Lett.* **279**, 67–76. <https://doi.org/10.1016/j.toxlet.2017.07.214> (2017).
59. Ross, B. M. et al. Decreased activity of brain phospholipid metabolic enzymes in human users of cocaine and methamphetamine. *Drug Alcohol Depend.* **67**, 73–79. [https://doi.org/10.1016/s0376-8716\(02\)00022-4](https://doi.org/10.1016/s0376-8716(02)00022-4) (2002).
60. Ross, B. M. & Turenne, S. D. Chronic cocaine administration reduces phospholipase A(2) activity in rat brain striatum. *Prostaglandins Leukot. Essent. Fat. Acids.* **66**, 479–483. <https://doi.org/10.1054/plef.2002.0385> (2002).
61. Feier, G. et al. Behavioral changes and brain energy metabolism dysfunction in rats treated with methamphetamine or dextroamphetamine. *Neurosci. Lett.* **530**, 75–79. <https://doi.org/10.1016/j.neulet.2012.09.039> (2012).
62. Estler, C. J. & Ammon, H. P. Modification by two beta-adrenergic blocking drugs of the effects of methamphetamine on behaviour and brain metabolism of mice. *J. Neurochem.* **18**, 777–779. <https://doi.org/10.1111/j.1471-4159.1971.tb12007.x> (1971).
63. Stephans, S. E., Whittingham, T. S., Douglas, A. J., Lust, W. D. & Yamamoto, B. K. Substrates of energy metabolism attenuate methamphetamine-induced neurotoxicity in striatum. *J. Neurochem.* **71**, 613–621. <https://doi.org/10.1046/j.1471-4159.1998.71020613.x> (1998).
64. Shima, N. et al. Influences of methamphetamine-induced acute intoxication on urinary and plasma metabolic profiles in the rat. *Toxicology.* **287**, 29–37. <https://doi.org/10.1016/j.tox.2011.05.012> (2011).
65. Bu, Q. et al. NMR-based metabolicomic in hippocampus, nucleus accumbens and prefrontal cortex of methamphetamine-sensitized rats. *Neurotoxicology.* **36**, 17–23. <https://doi.org/10.1016/j.neuro.2013.02.007> (2013).
66. Lin, M. et al. Metabolomics profiling of methamphetamine addicted human serum and three rat brain areas. *RSC Adv.* **9**, 41107–41119. <https://doi.org/10.1039/c9ra08096a> (2019).
67. Marcos, A. et al. The effects of combined intravenous cocaine and ethanol self-administration on the behavioral and amino acid profile of young adult rats. *PLoS One.* **15**, e0227044. <https://doi.org/10.1371/journal.pone.0227044> (2020).
68. Mews, P. et al. Convergent abnormalities in striatal gene networks in human cocaine use disorder and mouse cocaine administration models. *Sci. Adv.* **9**, eadd8946. <https://doi.org/10.1126/sciadv.add8946> (2023).
69. Campbell, U. C. & Carroll, M. E. Acquisition of drug self-administration: environmental and pharmacological interventions. *Exp. Clin. Psychopharmacol.* **8**, 312–325. <https://doi.org/10.1037/1064-1297.8.3.312> (2000).
70. Montague, P. R., Gancayco, C. D., Winn, M. J., Marchase, R. B. & Friedlander, M. J. Role of NO production in NMDA receptor-mediated neurotransmitter release in cerebral cortex. *Science.* **263**, 973–977. <https://doi.org/10.1126/science.7508638> (1994).
71. Sandor, N. T., Brassai, A., Puskas, A. & Lendvai, B. Role of nitric oxide in modulating neurotransmitter release from rat striatum. *Brain Res. Bull.* **36**, 483–486. [https://doi.org/10.1016/0361-9230\(94\)00229-t](https://doi.org/10.1016/0361-9230(94)00229-t) (1995).
72. Motahari, A. A., Sahraei, H. & Meftahi, G. H. Role of nitric oxide on dopamine release and morphine-dependency. *Basic. Clin. Neurosci.* **7**, 283–290. <https://doi.org/10.15412/j.Bcn.03070401> (2016).
73. Centonze, D., Gubellini, P., Pisani, A., Bernardi, G. & Calabresi, P. Dopamine, acetylcholine and nitric oxide systems interact to induce corticostriatal synaptic plasticity. *Rev. Neurosci.* **14**, 207–216. <https://doi.org/10.1515/revneuro.2003.14.3.207> (2003).
74. Hardingham, N., Dachtler, J. & Fox, K. The role of nitric oxide in pre-synaptic plasticity and homeostasis. *Front. Cell. Neurosci.* **7**, 190. <https://doi.org/10.3389/fncel.2013.00190> (2013).

75. Masood, A., Banerjee, B., Vijayan, V. K. & Ray, A. Modulation of stress-induced neurobehavioral changes by nitric oxide in rats. *Eur. J. Pharmacol.* **458**, 135–139. [https://doi.org/10.1016/s0014-2999\(02\)02688-2](https://doi.org/10.1016/s0014-2999(02)02688-2) (2003).
76. Malinski, T. Nitric oxide and nitroxidative stress in Alzheimer's disease. *J. Alzheimers Dis.* **11**, 207–218. <https://doi.org/10.3233/jad-2007-11208> (2007).
77. Collins, S. L. & Kantak, K. M. Neuronal nitric oxide synthase inhibition decreases cocaine self-administration behavior in rats. *Psychopharmacol. (Berl.)* **159**, 361–369. <https://doi.org/10.1007/s00213-001-0935-8> (2002).
78. Orsini, C., Izzo, E., Koob, G. F. & Pulvirenti, L. Blockade of nitric oxide synthesis reduces responding for cocaine self-administration during extinction and reinstatement. *Brain Res.* **925**, 133–140. [https://doi.org/10.1016/s0006-8993\(01\)03267-x](https://doi.org/10.1016/s0006-8993(01)03267-x) (2002).
79. Sahraei, H. et al. Effects of nitric oxide on morphine self-administration in rat. *Pharmacol. Biochem. Behav.* **77**, 111–116. <https://doi.org/10.1016/j.pbb.2003.10.008> (2004).
80. Smith, A. C. W. et al. Accumbens nNOS interneurons regulate cocaine relapse. *J. Neurosci.* **37**, 742–756. <https://doi.org/10.1523/jneurosci.2673-16.2016> (2017).
81. Cloak, C. C., Alicata, D., Chang, L., Andrews-Shigaki, B. & Ernst, T. Age and sex effects levels of choline compounds in the anterior cingulate cortex of adolescent methamphetamine users. *Drug Alcohol Depend.* **119**, 207–215. <https://doi.org/10.1016/j.drugalcdep.2011.06.017> (2011).
82. Salo, R. et al. Extended findings of brain metabolite normalization in MA-dependent subjects across sustained abstinence: a proton MRS study. *Drug Alcohol Depend.* **113**, 133–138. <https://doi.org/10.1016/j.drugalcdep.2010.07.015> (2011).
83. Ruda-Kucrova, J. et al. Sex differences in the reinstatement of methamphetamine seeking after forced abstinence in Sprague-Dawley rats. *Front. Psychiatry.* **6**, 91. <https://doi.org/10.3389/fpsyg.2015.00091> (2015).
84. Job, M. O., Chojnacki, M. R., Daiwile, A. P. & Cadet, J. L. Chemogenetic inhibition of dopamine D1-expressing neurons in the dorsal striatum does not alter methamphetamine intake in either male or female long Evans rats. *Neurosci. Lett.* **729**, 134987. <https://doi.org/10.1016/j.neulet.2020.134987> (2020).
85. Zlebnik, N. E. et al. Age-specific treatment effects of orexin/hypocretin-receptor antagonism on methamphetamine-seeking behavior. *Drug Alcohol Depend.* **224**, 108719. <https://doi.org/10.1016/j.drugalcdep.2021.108719> (2021).
86. Gonçalves, J. et al. Extended-access methamphetamine self-administration elicits neuroinflammatory response along with blood-brain barrier breakdown. *Brain Behav. Immun.* **62**, 306–317. <https://doi.org/10.1016/j.bbi.2017.02.017> (2017).
87. Everett, N. A., Baracz, S. J. & Cornish, J. L. The effect of chronic oxytocin treatment during abstinence from methamphetamine self-administration on incubation of craving, reinstatement, and anxiety. *Neuropsychopharmacology.* **45**, 597–605. <https://doi.org/10.1038/s41386-019-0566-6> (2020).
88. Westbrook, S. R., Dwyer, M. R., Cortes, L. R. & Gulley, J. M. Extended access self-administration of methamphetamine is associated with age- and sex-dependent differences in drug taking behavior and recognition memory in rats. *Behav. Brain Res.* **390**, 112659. <https://doi.org/10.1016/j.bbr.2020.112659> (2020).
89. Sharma, A., Harutyunyan, A., Schneider, B. L. & Moszczynska, A. Parkin regulates drug-taking behavior in rat model of methamphetamine use disorder. *Transl. Psychiatry.* **11**, 293. <https://doi.org/10.1038/s41398-021-01387-7> (2021).
90. Vollmer, K. M. et al. A novel assay allowing drug self-administration, extinction, and reinstatement testing in Head-restrained mice. *Front. Behav. Neurosci.* **15**, 744715. <https://doi.org/10.3389/fnbeh.2021.744715> (2021).

## Acknowledgements

This research was supported by the Basic Science Research Program through the National Research Foundation of Korea (NRF) and was funded by the Ministry of Education (NRF-2016R1A6A1A03011325 and RS-2023-00242428).

## Author contributions

Sang-Hoon Song: Methodology, Formal analysis, Writing - original draft, Visualization. Suji Kim: Methodology, Formal analysis, Writing original draft. Won-Jun Jang: Formal analysis, Visualization. In Soo Ryu: Investigation, Formal analysis. Chul-Ho Jeong: Conceptualization, Supervision, Writing - review & editing. Sooyeon Lee: Conceptualization, Supervision, Writing - review & editing.

## Declarations

### Competing interests

The authors declare no competing interests.

### Ethics statement

All animal procedures performed during this study were reviewed and approved by the Institutional Animal Care and Use Committee of the Korea Institute of Toxicology.

### Additional information

**Supplementary Information** The online version contains supplementary material available at <https://doi.org/10.1038/s41598-024-73247-5>.

**Correspondence** and requests for materials should be addressed to C.-H.J. or S.L.

**Reprints and permissions information** is available at [www.nature.com/reprints](http://www.nature.com/reprints).

**Publisher's note** Springer Nature remains neutral with regard to jurisdictional claims in published maps and institutional affiliations.

**Open Access** This article is licensed under a Creative Commons Attribution-NonCommercial-NoDerivatives 4.0 International License, which permits any non-commercial use, sharing, distribution and reproduction in any medium or format, as long as you give appropriate credit to the original author(s) and the source, provide a link to the Creative Commons licence, and indicate if you modified the licensed material. You do not have permission under this licence to share adapted material derived from this article or parts of it. The images or other third party material in this article are included in the article's Creative Commons licence, unless indicated otherwise in a credit line to the material. If material is not included in the article's Creative Commons licence and your intended use is not permitted by statutory regulation or exceeds the permitted use, you will need to obtain permission directly from the copyright holder. To view a copy of this licence, visit <http://creativecommons.org/licenses/by-nc-nd/4.0/>.

© The Author(s) 2024